Universidad del País Vasco
Euskal Herriko Unibertsitatea

ZTF-FCT
Zientzia eta Teknologia Fakultatea
Facultad de Ciencia y Tecnología

Euskadi 2006

FACULTAD DE CIENCIA Y TECNOLOGÍA. LEIOA

TRABAJO FIN DE GRADO BIOTECNOLOGÍA

FTIR CHARACTERIZATION OF STRESS RESPONSE TO ACETIC ACID IN *SACCHAROMYCES CEREVISIAE* CELLS. ROLE OF MCR1 TO COUNTERACT THE OXIDATIVE STRESS.

Alumno: ***Rodríguez Carranza, María***
Fecha: Junio 2016

Director
Dra. María Asunción Requero Zabala

Tutor
Dra. Diletta Ami (Università degli Studi di Milano-Bicocca)

Curso Académico
2015/2016

TABLE OF CONTENTS

SUMMARY

Saccharomyces cerevisiae cells are widely employed as microbial factories for the production of bioethanol through the alcoholic fermentation. One of the main bottlenecks of the process is the formation of toxic metabolites, such as acetic acid, that can inhibit the production pathway.

In order to increase the final yield, the biotechnology industry is looking for the optimal conditions to carry out the fermentation process.

In this project, we studied the infrared response of *S. cerevisiae* cells exposed to acetic acid. In particular, we investigated whether the overexpression of MCR1 - a gene involved in the response to oxidative stress - makes the cells more resistant to the acetic acid. We found that in the exponential phase of growth cells engineered with the MCR1 seem to counteract the effects of acetic acid by decreasing membrane fluidity, mainly through the dramatic reduction of phosphatidylcholine and the increase of ergosterol. However, interestingly, in the stationary phase of growth the MCR1 gene seemed to be mainly involved in the prevention of oxidative stress due to aging.

1. INTRODUCTION

In recent years, the biotechnology industry is looking for improvements in the production of bioethanol as biofuel. Indeed, due to the crisis of fossil fuels, bioethanol consumption dramatically increased in the last decade.

S. cerevisiae cells produce ethanol through the alcoholic fermentation. A main bottleneck of this process is the formation of toxic metabolites, such as acetic acid, that can cause the inhibition of the production pathway. For this reason, it is crucial to better understand the mechanisms of acetic toxicity, in order to finally design the optimal conditions to carry out the alcoholic fermentation. In addition, engineered strains of *S. cerevisiae* are developed in order to make the cells more robust against toxic metabolites (Wallace-Salinas *et al,.* 2014).

Recent studies demonstrated that the protein encoded by MCR1 gene, mitochondrial NADH-cytochrome b_5 reductase, plays a key role in the response to oxidative damage in *S. cerevisiae* and overexpression of this gene makes the cells more resistant against oxidative stress (Lee *et al.,* 2001). This gene encodes two isoforms of the mitochondrial NADH- cytochrome b_5 reductase: one form is located in the outer membrane, while the other is in the intermembrane space (Meineke *et al.,* 2008). In this study, we analyzed by Fourier transform infrared (FTIR) microspectroscopy intact *S. cerevisiae* cells belonging to an evolved strain (our control), and to the MCR1 engineered strain, to investigate whether the MCR1 overexpression makes the cells more resistant to acetic acid.

FTIR microspectroscopy is in a non-invasive and label-free technique that allows to obtain a molecular fingerprint of the sample under investigation, including intact cells, tissues and whole model organisms. This spectroscopy tool provides a characterization of the composition and structure of the main cellular biomolecules, such as proteins, lipids, nucleic acids and carbohydrates, making it possible the in situ investigation of biological processes. In particular, the use of an infrared microscope makes it possible to measure the infrared (IR) absorption spectra from a micro-volume of the sample, thanks to the variable aperture of the microscope that can be adjusted from ~ 250 µm x 250 µm down to 20 µm x 20 µm.

Since the FTIR spectra of intact cells are very complex, being due to the overlapping absorption of the different biomolecules, we employed second derivative analysis that allows to resolve, and therefore better assign, the different components of the large IR bands.

In particular, we compared the infrared response of *S. cerevisiae* evolved strains with that of MCR1 engineered cells, after treatment with acetic acid, in the exponential and stationary phases of growth.

Interestingly, we found that the overexpression of MCR1 leads to the increase of ergosterol synthesis – simultaneous to a dramatic decrease of phosphatidylcholine - that makes the membrane more compact, therefore limiting the acetic acid entrance. On the other hand, the strategy adopted by the not engineered cells to limit the effects of the stressing agent consisted in the increase of the acyl chain length, accompanied by a lower reduction of phosphatidylcholine and ergosterol. Noteworthy, in the stationary phase the effects of MCR1 overexpression seem to be mainly the limitation of protein aggregation due to aging.

2. MATERIALS AND METHODS

2.1. YEAST STRAINS AND KINETIC GROWTH

S. cerevisiae evolved strain was obtained from *S. cerevisiae* Ethanol Red strain and was able to grow on C5 carbohydrates through the introduction of the bacterial pathway for the xylose consumption. This strain was transformed to overexpress *MCR1*.

Pre-inoculum. *S. cerevisiae* cells were pre-inoculated in oxygenated glass tubes containing 4 mL of rich medium (YPD). Then, the tubes were placed under agitation at 160 rpm in the thermostatic chamber at 30°C until the cells were grown at least to the exponential phase.

Inoculum. Inoculum was prepared in flasks containing modified Verduyn medium in a quantity equal to one fifth of the maximum capacity of the flasks.

Inoculum was made in a variable optical density depending on the kinetic used. For these experiments we employed OD_{660} equal to 0.1 for the inoculum. Then, the cells grew in agitation at 160 rpm and at 30°C. After 6 hours in *S. cerevisiae* and 24 hours in *S. cerevisiae* treated with acetic acid the cells reached exponential phase (OD_{660}= 0.4-0.55). *S. cerevisiae* were in stationary phase after 48 hours, however the cells treated with acetic acid reached the stationary phase in 72 hours (OD_{660}= 9.2-9-5).

Table 1. The employed $OD_{660\ nm}$ for each phase of growth of S. Cerevisiae cells. The measurements were made by the spectrophotometer (Shimadzu UV-1601).

Phase of Growth	**S. cerevisiae**		**S. cerevisiae + Acetic acid**	
	CONTROL	MCR1	CONTROL	MCR1
Inoculum	0.099	0.097	0.097	0.098
Exponencial	0.4	0.45	0.52	0.55
Stationary	9.2	9.5	9.3	9.4

For the treatment with the oxidative agent, the acetic acid was added in the preparation of the mediums. The employed concentration was 50 mM of acetic acid.

2.2. FTIR MICROSPECTROSCOPY ANALYSIS

S. cerevisiae cells at exponential and stationary phases were washed three times in distilled water to eliminate medium contamination. Approximately 3 µl of the cell suspension were deposited into an IR transparent BaF_2 support and dried at room temperature for at least 30 minutes to eliminate the excess water.

FTIR absorption spectra were acquired in transmission mode, between 4000 and 700 cm^{-1}, by means of a Varian 610-IR infrared microscope coupled to the Varian 610-IR FTIR spectrometer (both from Varian Australia Pty Ltd), equipped with a mercury cadmium telluride (MCT) nitrogen-cooled detector. The variable microscope aperture was adjusted to 100 µm X 100 µm. Measurements were performed at 2 cm^{-1} spectral resolution; 25 KHz scan speed, triangular apodization, and by the accumulation of 512 scan co-additions.

Second-derivatives spectra were obtained following the Savitsky-Golay method (third-grade polynomial, 9 smoothing points) after a binomial 13 smoothing points of the measured spectra, using the GRAMS/32 software (Galactic Industries Corporation, USA).

To verify the reproducibility and reliability of the spectral results, more than three independent preparations were analyzed and for each preparation at least ten spectra for sample were measured.

3. RESULTS

In **Figure 1** the measured FTIR spectrum of *S. cerevisiae* intact cells is reported. As illustrated, the spectrum is complex since it is due to the absorption of the different biomolecules (Ami *et al*, 2012).

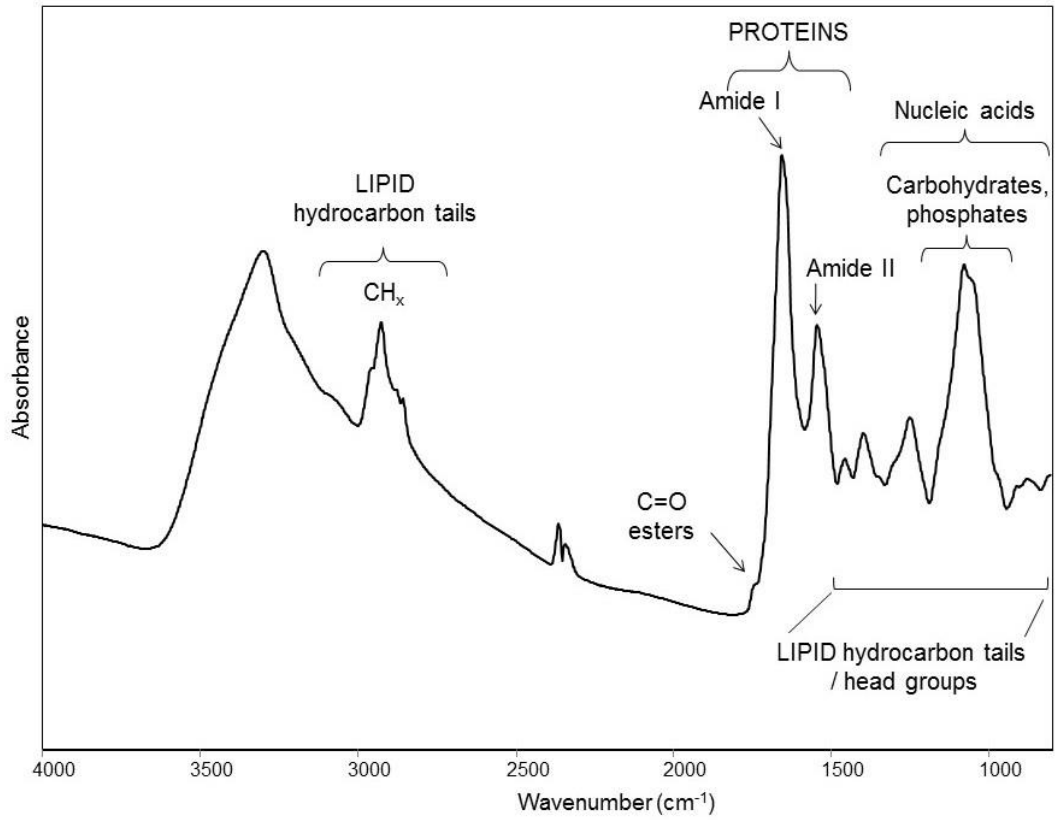

Figure 1. **FTIR absorption spectrum of *S. cerevisiae* intact cells.** The measured FTIR spectrum of the *S. cerevisiae* evolved strain cells is displayed. The assignment of selected absorption to the main biomolecules is reported.

In particular, the lipid hydrocarbon tails absorb between 3050 and 2800 cm^{-1} and between 1500 and 1350 cm^{-1}, where also the lipid head group absorption occurs, while around 1740 cm^{-1} the ester carbonyl IR response is observed (Casal and Mantsch, 1984; Arrondo and Goñi, 1998). In addition, between 1700 and 1500 cm^{-1} the spectrum is dominated by the amide I and amide II bands, respectively due to the C=O stretching and the NH bending of the peptide bond. In particular, the amide I band gives information on the protein secondary structures and aggregation (Tamm and Tatulian, 1997; Seshadri *et al.*, 1999; Barth, 2007). Furthermore, the spectral range between 1250 and 900 cm^{-1} is dominated by the absorption of phosphate groups mainly from

phospholipids and nucleic acids, as well as by the C-O absorption of carbohydrates (Casal and Mantsch, 1984; Kacurakova and Mathlouthi, 1996; Banyay *et al.,* 2003).

In this study, we investigated the infrared absorption of *S. cerevisiae* evolved strain and of the engineered strain with MCR1, after treatment with acetic acid and under control condition (without acetic acetic). In particular, we compared cells stressed with acetic acid with untreated cells to explore possible cell biomolecule changes induced by the exposure to the stressing agent. The measurements were performed by FTIR microspectroscopy, on cells in the exponential and stationary phases of growth.

3.1. SECOND DERIVATIVE ANALYSIS OF THE *S. cerevisiae* EVOLVED STRAIN TREATED WITH ACETIC ACID: EXPONENTIAL PHASE

To better evaluate possible spectral changes occurring after cell treatment with acetic acid, we analyzed the second derivatives of the FTIR absorption spectra, since they enable to resolve the overlapping components of the IR absorption bands (Susi *et al,* 1986).

In **Figure 2** we compared the IR response of *S. cerevisiae* evolved strain cells treated with acetic acid with that of untreated cells, in the amide I region.

As displayed, the second derivative spectrum of the control cells is characterized by two main spectral components at ~1656 cm^{-1} due to alpha helix and random coil structures of the whole cell proteins and at ~ 1638 cm^{-1} mainly due to intramolecular native beta sheets (Barth, 2007). Two minor components at ~ 1691 cm^{-1} and ~ 1685 cm^{-1} have been observed, assigned to intramolecular native beta sheets and beta turns, respectively (Tamm and Tatulian, 1997; Barth, 2007). These spectral features were found to change after acetic acid cell treatment. In particular, we found a slight intensity increase of the alpha helix and random coil band accompanied by an important intensity decrease of the native beta sheet component. In addition, a shoulder of the 1638 cm^{-1} band appeared around 1625 cm^{-1} that can be assigned to intermolecular beta sheets typical of protein aggregates (Seshadri *et al.,* 1999).

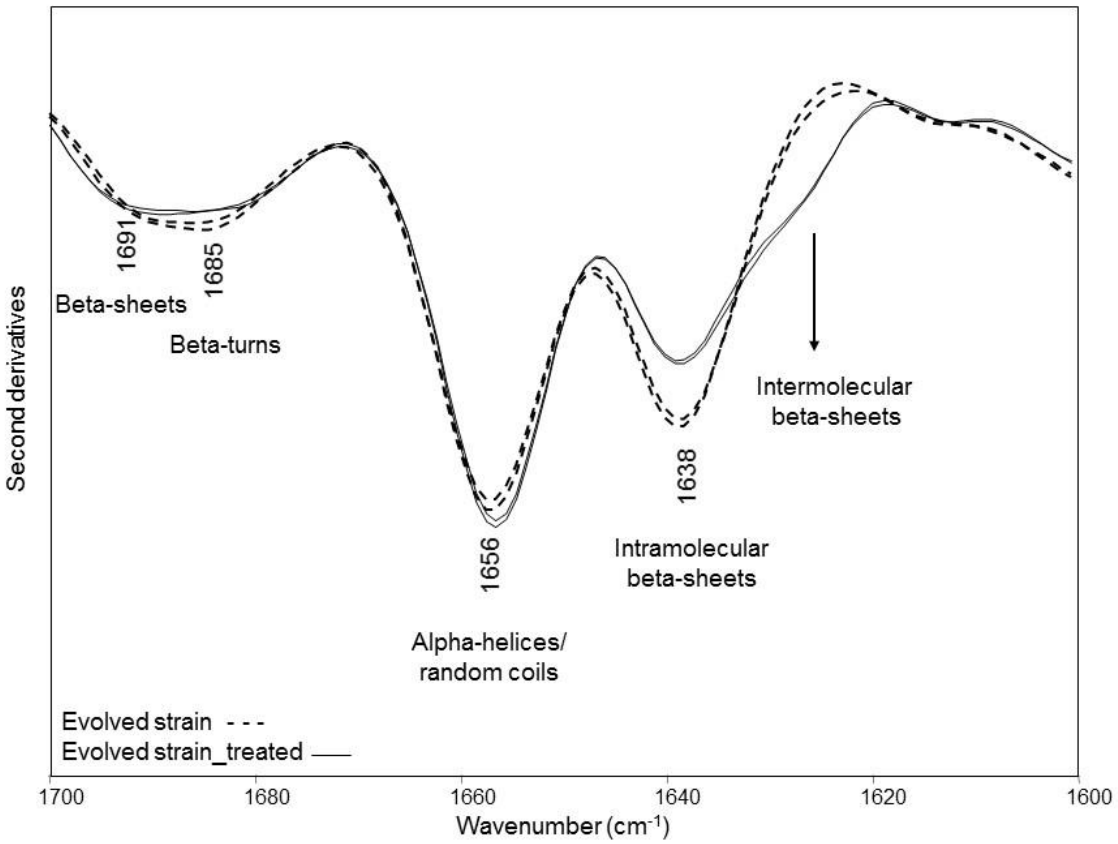

Figure 2. Second derivative spectra of the amide I region of S. cerevisiae evolved strain in exponential phase. Second derivative spectra have been obtained after normalization of the absorption spectra at the amide I band area. Two representative spectra for each sample have been reported.

Furthermore, as reported in **Figure 3**, we analyzed the second derivative spectra in the 1500-1200 cm^{-1} region, dominated by the absorption of lipid hydrocarbon tails and head groups, as well as of phosphates.

In particular, the second derivative spectrum of control cells is characterized by a number of well resolved bands mainly due to the CH_2 and CH_3 deformation modes of lipid hydrocarbon tails and head groups (Casal and Mantsch, 1984; Arrondo and Goñi, 1998). In particular, the ~ 1467 cm^{-1} band is due to the overlapping absorption of CH_2 and CH_3, while the ~ 1455 cm^{-1}, ~ 1439 cm^{-1} and 1368 cm^{-1} bands are due to CH_3; furthermore, the 1416 cm^{-1} absorption is due to CH_2, while the component at ~ 1396 cm^{-1} can be mainly assigned to the CH_3 of the $N(CH_3)_3$ group, typical of choline. In addition, the band at ~ 1386 cm^{-1} is due to the absorption of CH_3 mainly from ergosterol (Levchuk, 1968). Finally, the broad band around 1247 cm^{-1} is mainly due to the PO_2^- group of phospholipids (Casal and Mantsch, 1984) with a contribution also

from nucleic acids (Banyay *et al.*, 2003). Interestingly, some of these spectral features were found to change after acetic acid treatment and in particular, we observed an upshift of the ~ 1396 cm^{-1} band to ~ 1400 cm^{-1}, that also decreased in intensity. Simultaneously, also a minor but significant reduction of the ~ 1386 cm^{-1} band occurred, that can be partly due to ergosterol. We should also note that the intensity reduction of the PO_2^- band also downshifted of a few cm^{-1}. Overall, these results suggest a possible reorganization of membrane lipids in cells exposed to the stressing agent.

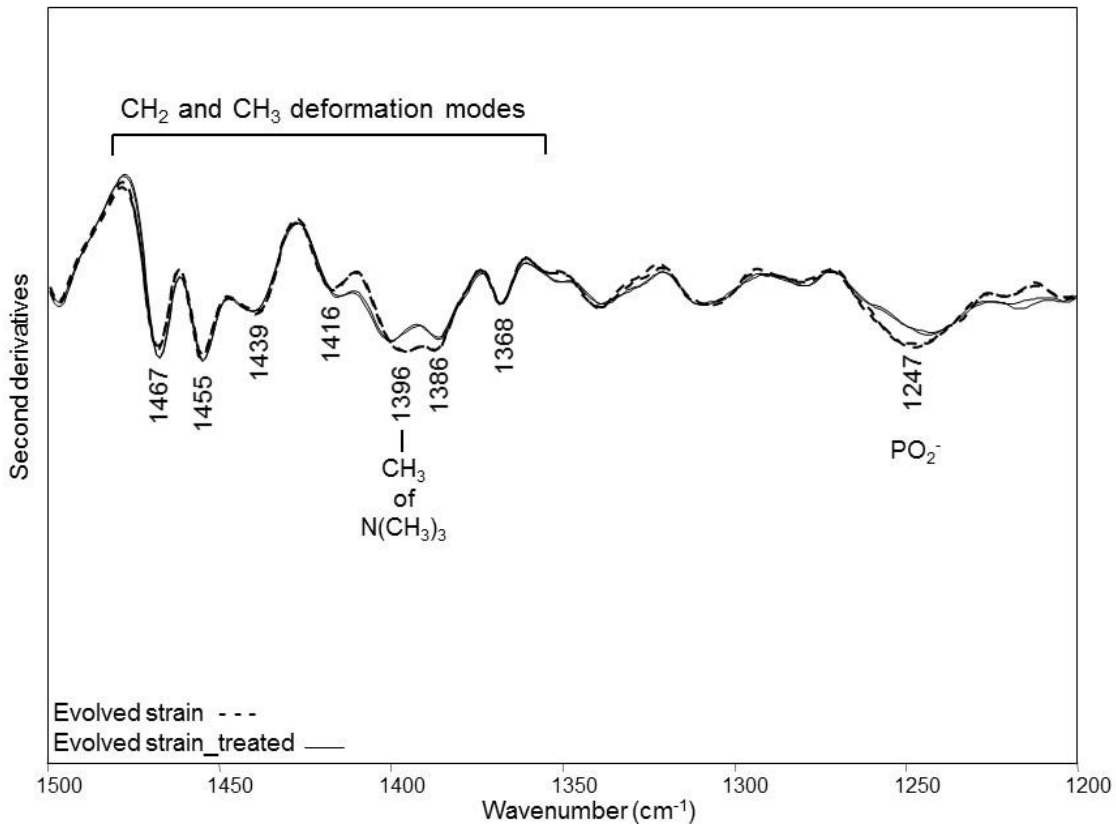

Figure 3. Second derivative analysis of the 1500-1200 cm^{-1} region of *S. cerevisiae* evolved strain in exponential phase. Second derivative spectra have been reported in the absorption range mainly due to lipid hydrocarbon tails and head groups, after normalization of the absorption spectra at the Amide I band area. Two representative spectra for each sample have been reported.

To better explore the cell lipid response, we analyzed the CH_2 and CH_3 stretching region, between 3050-2800 cm^{-1}. In particular, as reported in **Figure 4**, the second derivative spectrum of control cells was characterized by four intense bands due to the absorption of CH_3 (at ~ 2958 and 2872 cm^{-1}) and CH_2 (at ~ 2921 and 2851 cm^{-1}) groups mainly of the lipid hydrocarbon tails (Casal *et al.*, 1984; Arrondo and Goñi,

1998). In addition, a shoulder around 2935 cm^{-1} is also detected, that can be mainly assigned to CH_2 stretching (Levchuk, 1968).To evaluate possible changes in hydrocarbon tail length and, therefore, a modification of membrane fluidity occurring after the acetic acid treatment, we normalized the second derivative spectra to the CH_3 band at 2958 cm^{-1}. In this way, we observed a slight increase in intensity of the CH_2 stretching band at ~ 2851 cm^{-1} after the acid treatment, that - in agreement with what found between 1500-1200 cm^{-1} - , could indicate a partial rearrangement of the hydrocarbon tails to counteract the exposure to the stressing agent. Moreover, the shoulder around 2935 cm^{-1} is less resolved compared to untreated cells.

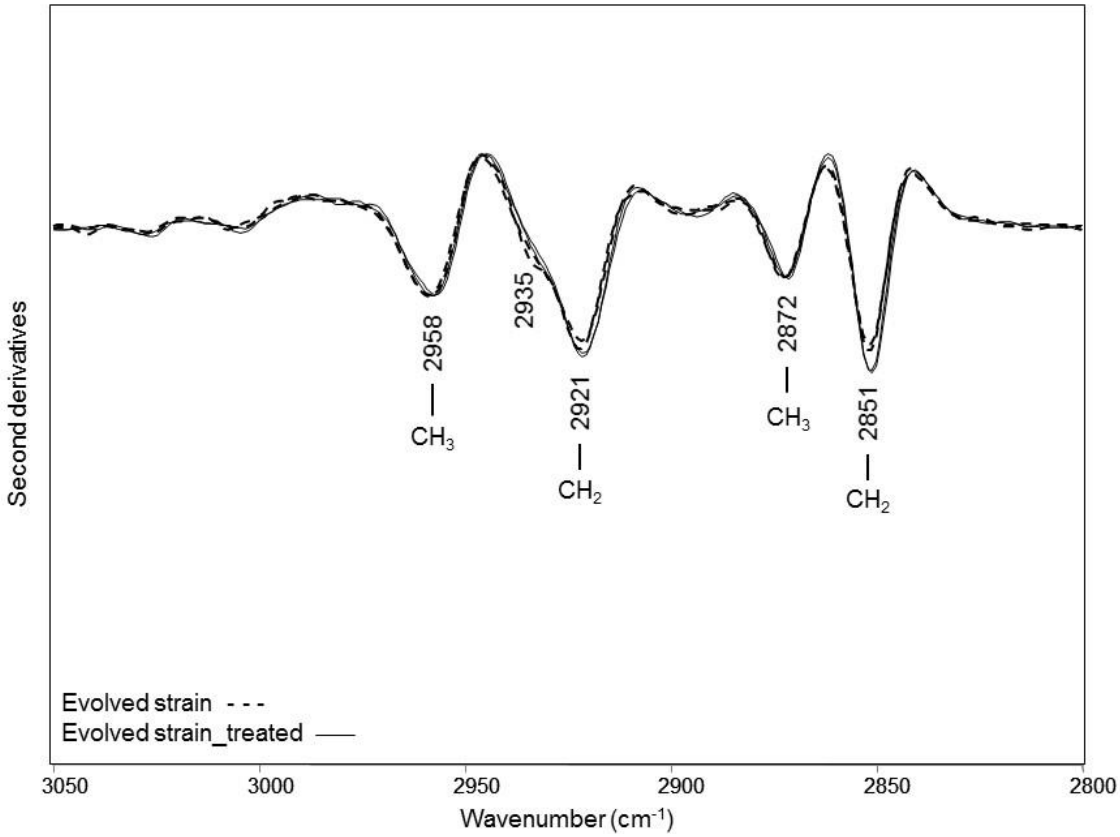

Figure 4. Second derivative analysis of the 3050-2800 cm^{-1} region of *S. cerevisiae* evolved strain in exponential phase. Second derivative spectra have been reported in the absorption range mainly due to CH_3 and CH_2 stretching vibrations of lipid hydrocarbon tails, after normalization of the absorption spectra at the CH_3 band at 2958 cm^{-1}. Two representative spectra for each sample have been reported.

Finally, we analyzed the IR response of *S. cerevisiae* evolved strain in the spectral range between 1200-900 cm^{-1}, a very complex region mainly due to the overlapping absorption of carbohydrates (C-O), as well as nucleic acids and also lipids.

Interestingly, in the system under investigation this absorption region can provide information on cell wall properties that involve in particular the envelope carbohydrate composition. However, due to the high complexity of the absorption, we should note that a precise band assignment could be difficult.

In **Figure 5**, we reported for *S. cerevisiae* evolved strain mainly the absorption of the principal constituents of the cell wall, mannans and glucans (Lesage and Bussey, 2006). In particular, the β(1-3) glucans are the major constituent of the inner wall while the β(1-6) glucans link the components of the inner and outer wall (Galichet *et al.*, 2001; Zimkus *et al.*, 2013). We should also note that the simultaneous presence of the three absorption at ~1157 cm^{-1}, ~1083 cm^{-1} and ~1022 cm^{-1} could be indicative of the presence of glycogen (Naumann, 2000).

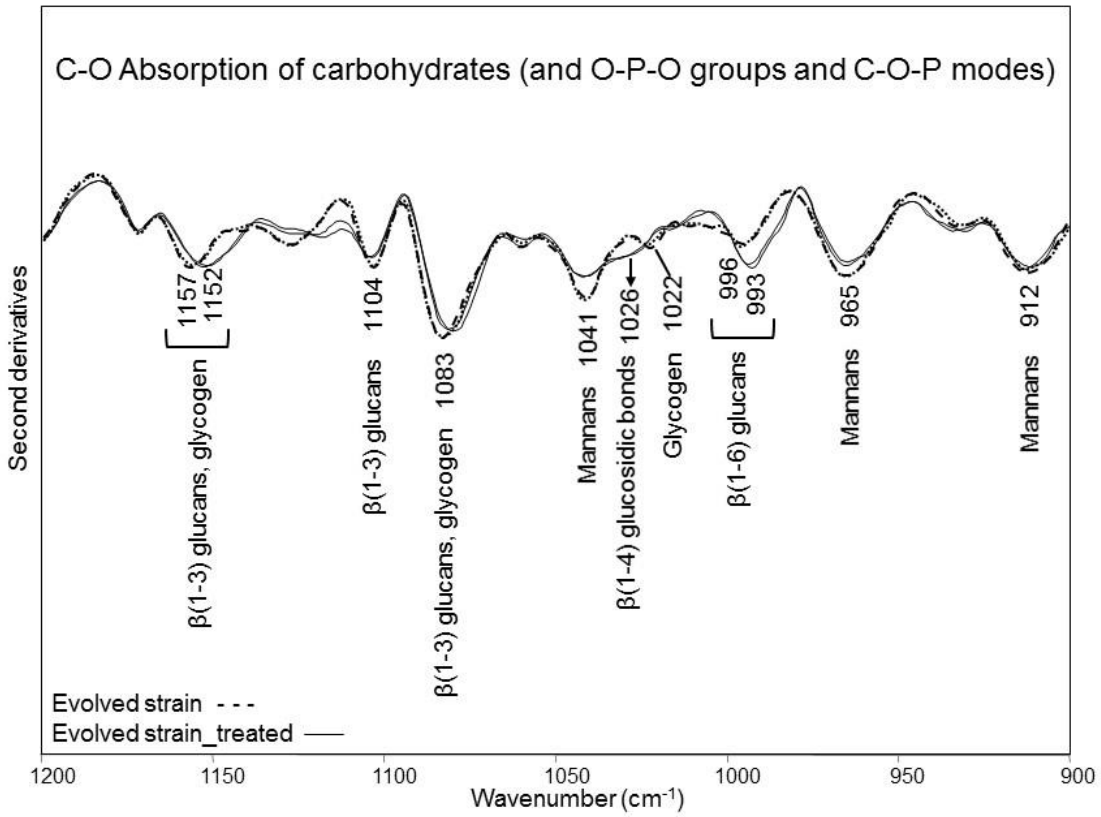

Figure 5. Second derivative analysis between 1200-900 cm^{-1} region of *S. cerevisiae* evolved strain in exponential phase. Second derivative spectra have been reported in the absorption range mainly due to carbohydrates, after normalization of the absorption spectra at the Amide I band area. Two representative spectra for each sample have been reported.

Interestingly, after acetic acid treatment the intensity of the bands due to β(1-3) glucans (1157, 1104 and 1083 cm^{-1}) and mannans (1041, 965 and 912 cm^{-1}) were found to decrease (Michell and Sourfield, 1969; Zimkus *et al.,* 2013). Moreover, we observed a downshift of the β(1-6) glucan band from 996 cm^{-1} band to 993 cm^{-1}, that increased also in intensity (Michell and Sourfield, 1969; Galichet *et al.,* 2001).

We also noted a shoulder around 1026 cm^{-1}, indicating an increase of the β(1-4) glucosidic bonds in chitin or in glucans linked to a N-acetylglucosamine molecule (Zimkus et al., 2013). Overall these results indicate that the exposure to acetic acid induced a few modifications of the cell wall properties.

3.2. SECOND DERIVATIVE ANALYSIS OF THE *S. cerevisiae* MCR1 ENGINEERED EVOLVED STRAIN TREATED WITH ACETIC ACID: EXPONENTIAL PHASE

In **Figure 6** we compared the IR response of the evolved strain engineered with MCR1, treated with acetic acid, with that of untreated cells, in the amide I region.

The second derivative spectrum of the MCR1 engineered cells is characterized by two main bands at ~1657 cm^{-1}, due to alpha helix and random coil structures of the whole cell proteins and at ~1638 cm^{-1}, mainly due to intramolecular native beta sheets (Barth, 2007). In addition, the two minor components at ~ 1690 cm^{-1} and at ~ 1685 cm^{-1} are due to intramolecular native beta sheets and beta turns, respectively (Tamm and Tatulian, 1997; Barth, 2007). These spectral features were found to partly change after acetic acid treatment. In particular, we observed an intensity decrease of the native beta sheet band at 1638 cm^{-1} that was accompanied by the appearance of a shoulder around 1625 cm^{-1}, assigned to intermolecular beta sheets typical of protein aggregates (Seshadri *et al.,* 1999).

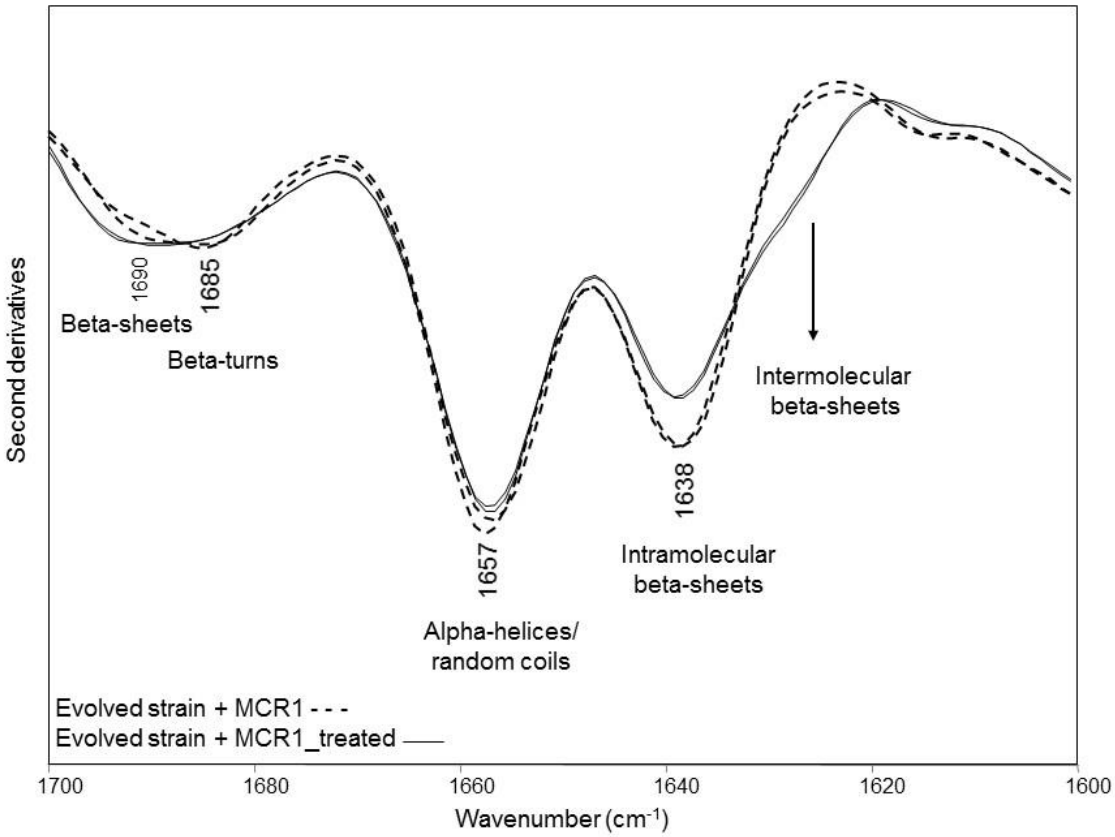

Figure 6. **Second derivative spectra of the amide I region of *S. cerevisiae* engineered evolved strain in exponential phase.** Second derivative spectra have been obtained after normalization of the absorption spectra at the amide I band area. Two representative spectra for each sample have been reported.

As discussed for the evolved strain (see **Figure 3**), in **Figure 7** we analyzed the lipid absorption between 1500- 1200 cm^{-1} groups. In addition to the components due to CH_3 and CH_2 groups of lipid hydrocarbon tails, the second derivative spectrum of the untreated MCR1 strain cells is characterized by the absorption at ~ 1396 cm^{-1}, mainly assigned to CH_3 of $N(CH_3)_3$ group typical of choline – and 1386 cm^{-1}, that we can mainly assign to ergosterol (Levchuk, 1968; Casal and Mantsch, 1984; Arrondo and Goñi, 1998). In addition, the band at ~ 1247 cm^{-1} is due to PO_2^- absorption (Casal and Mantsch, 1984; Banyay *et al.,* 2003). Interestingly, after acetic acid treatment, a significant intensity decrease of the 1396 cm^{-1} and 1247 cm^{-1} bands occurred, likely indicating a reduction in particular of phosphatidylcholine and a consequent reorganization of membrane phospholipids. On the contrary, the 1386 cm^{-1} component was not found to change in intensity after the treatment.

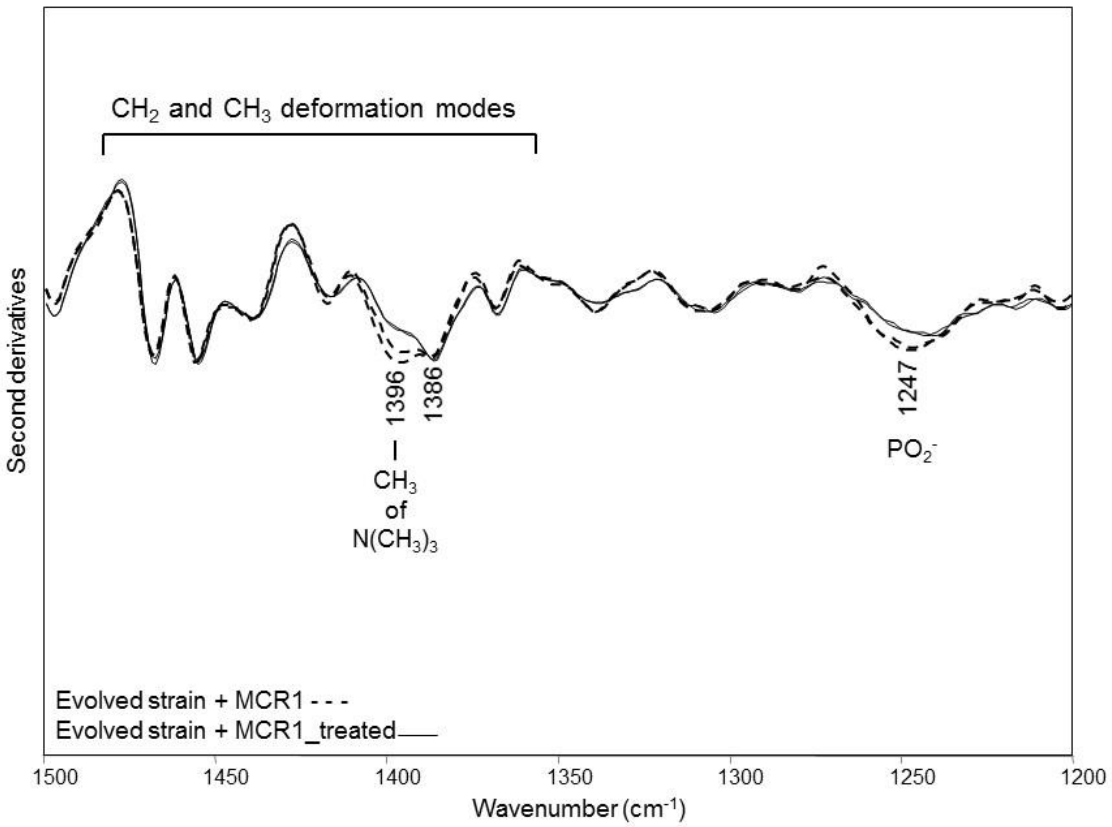

Figure 7. Second derivative analysis between 1500-1200 cm^{-1} of *S. cerevisiae* MCR1 engineered evolved strain in exponential phase. Second derivative spectra have been reported in the absorption range mainly due to lipid hydrocarbon tails and head groups, after normalization of the absorption spectra at the Amide I band area. Two representative spectra for each sample have been reported.

Furthermore, in **Figure 8** we analyzed the 3050-2800 cm^{-1} region, dominated by the CH_2 (at ~ 2921 and 2851 cm^{-1}) and CH_3 (at ~ 2958 and 2872 cm^{-1}) stretching vibrations mainly from lipid hydrocarbon tails (Casal and Mantsch, 1984; Arrondo and Goñi, 1998). As displayed, only a slight decrease of the CH_2 band at 2921 cm^{-1} was detected after the treatment with acetic acid. Notworthy, the shoulder at around 2935cm^{-1} displayed a similar intensity to that detected in untreated cells.

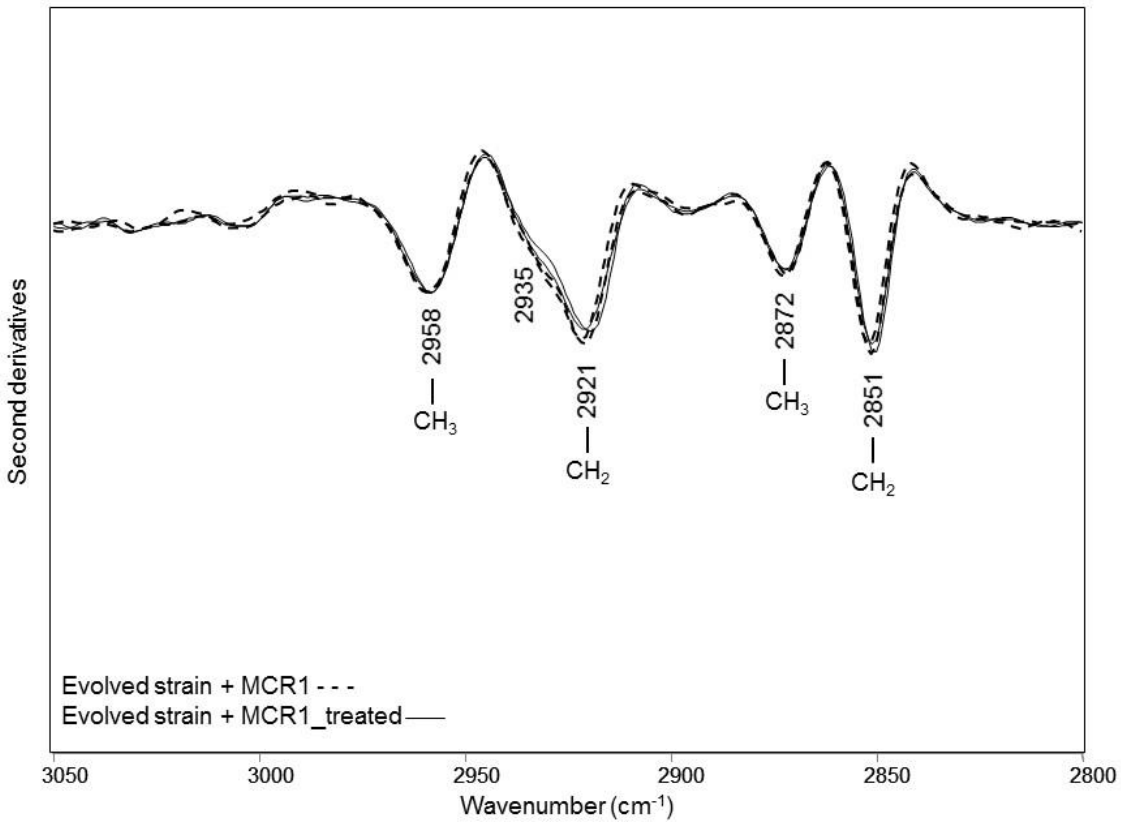

Figure 8. Second derivative analysis of the 3050-2800 cm^{-1} region of *S. cerevisiae* MCR1 engineered evolved strain in exponential phase. Second derivative spectra have been reported in the absorption range mainly due to CH_3 and CH_2 stretching vibrations of lipid hydrocarbon tails, after normalization of the absorption spectra at the CH_3 band at 2958 cm^{-1}. Two representative spectra for each sample have been reported.

Finally, in **Figure 9** we analyzed the carbohydrate absorption of *S. cerevisiae* MCR1 engineered cells. As described for the evolved strain (see **Figure 5**), we reported the main assignment for the untreated cells and - as it can be seen - the absorption is dominated by the carbohydrate components of the cell wall.

Compared to untreated cells, the acetic acid treatment caused an important variation of a few spectral features that suggests a modification of the chemical-physical properties of cell wall. In particular, a significant intensity reduction was observed for the absorption mainly due to β(1-3) glucans (~1156 cm^{-1} and ~1083 cm^{-1}) and to mannans (~1042 cm^{-1}). Furthermore, an intensity decrease of the β(1-6) glucan band at ~ 994 cm^{-1} was detected, accompanied by an intensity increase of the band at ~ 1023

cm^{-1} was also found, that can be assigned to β(1-4) glucosidic bonds (Galichet *et al.*, 2001; Zimkus *et al.*, 2013).

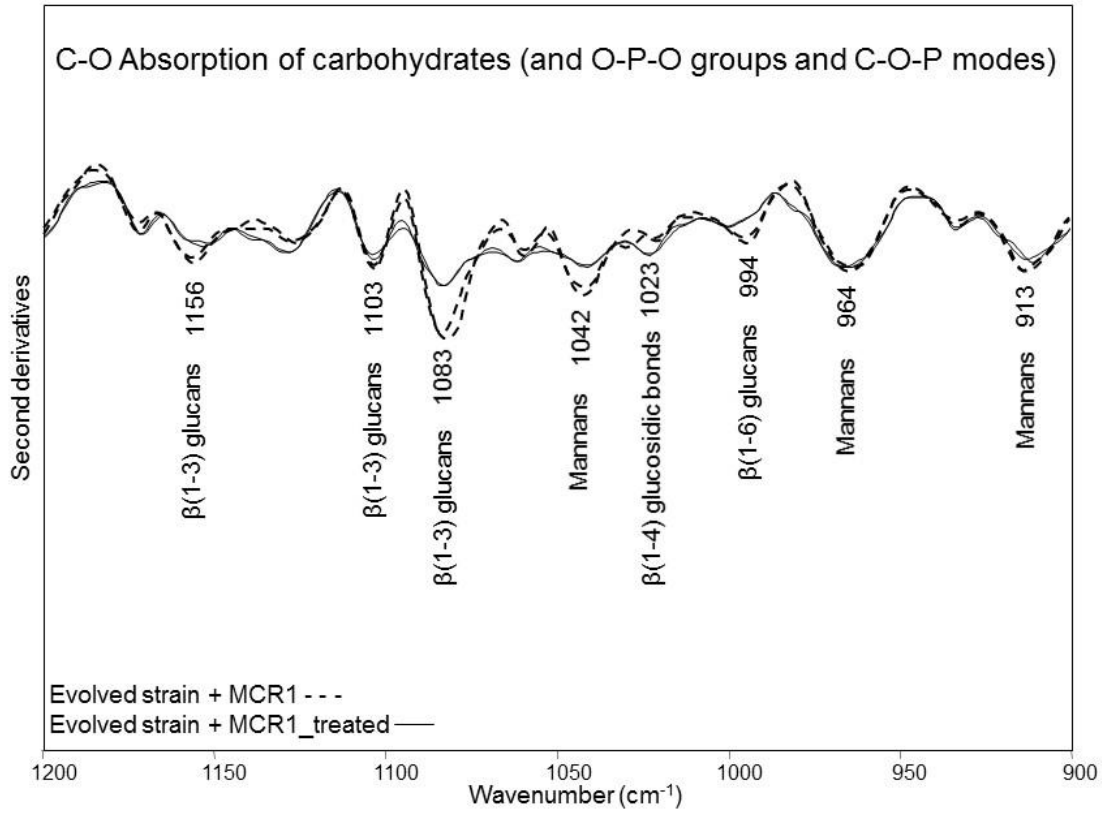

Figure 9. Second derivative analysis between 1200-900 cm^{-1} region of *S. cerevisiae* MCR1 engineered evolved strain in exponential phase. Second derivative spectra have been reported in the absorption range mainly due to carbohydrates, after normalization of the absorption spectra at the Amide I band area. Two representative spectra for each sample have been reported.

3.3. SECOND DERIVATIVE ANALYSIS OF THE *S. cerevisiae* evolved STRAIN TREATED WITH ACETIC ACID: STATIONARY PHASE

In **Figure 10** the infrared response of the *S. cerevisiae* evolved strain cells treated with acetic acid - in the stationary phase of growth - is compared with that of untreated cells in the amide I region.

In particular, the second derivative spectrum of the *S. cerevisiae* evolved strain is characterized by three main spectral components: ~1656 cm^{-1}, due to alpha helix and random coil structures of the whole cell proteins; ~ 1638 cm^{-1} mainly due to intramolecular native beta sheets (Tamm and Tatulian, 1997; Barth, 2007) and ~ 1628

cm^{-1} band, due to intermolecular beta sheets typical of protein aggregates (Seshadri *et al.*, 1999). The presence in the control cells of this component could be a consequence of cell aging, in particular as the result of a decrease of cell proteolysis possibly causing the protein unfolding (Squier, 2001 and Chen *et al.*, 2005).

Furthermore, the two absorption respectively at ~ 1690 cm^{-1} and ~ 1680 cm^{-1} were also detected, due to intramolecular / intermolecular beta sheets and beta turns, respectively. The treatment with acetic acid led to a few changes of these spectral features, as expected. In particular, we observed an important intensity reduction of the intramolecular native beta sheet band at ~ 1638 cm^{-1}, accompanied by a significant increase of the intermolecular beta sheet band at ~ 1628 cm^{-1}. Simultaneously, the intermolecular beta sheet component at 1694 cm^{-1} also appeared. Overall these results indicate the formation of new protein aggregates, compared to untreated cells, as a consequence of acetic acid treatment.

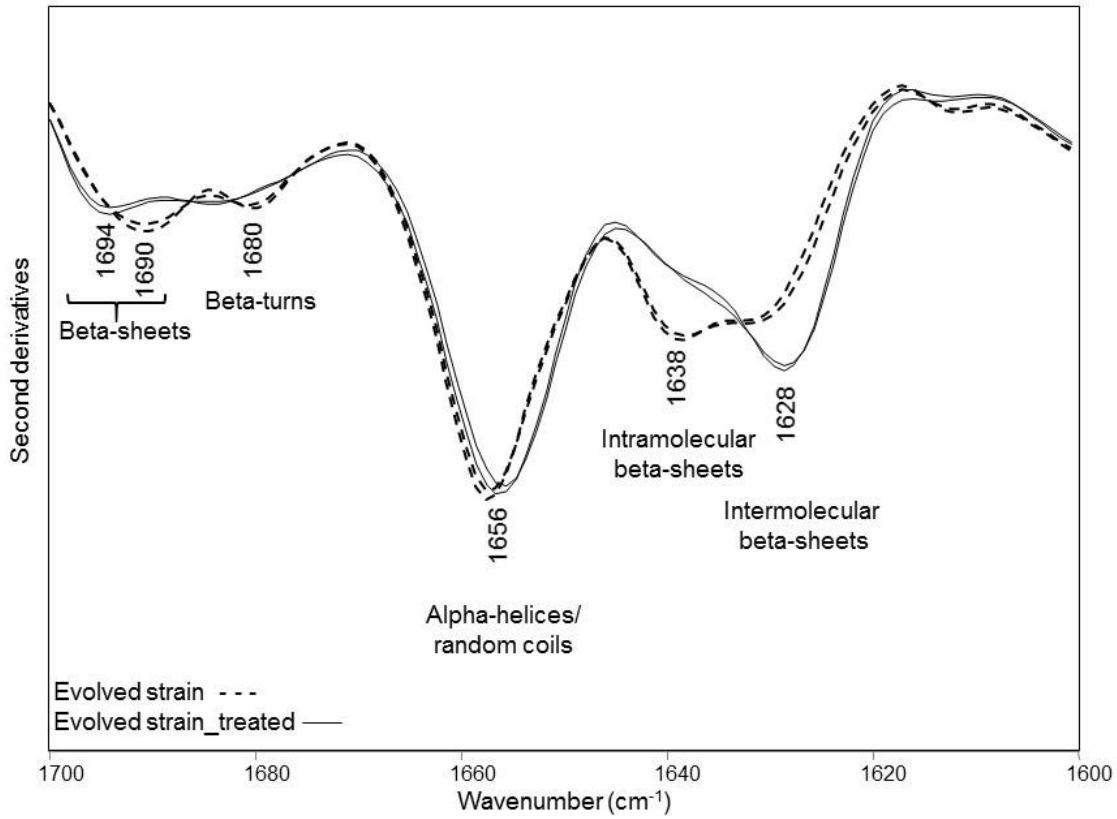

Figure 10. Second derivative spectra of the Amide I region of *S. cerevisiae* evolved strain in stationary phase. Second derivative spectra have been obtained after normalization of the absorption spectra at the amide I band area. Two representative spectra for each sample have been reported.

The second derivatives analysis between 1500-1200 cm^{-1}, reported in **Figure 11**, indicated that acetic acid treatment induced a slight but significant reduction in particular of the ~ 1400 cm^{-1}, that suggests a reduction mainly of phosphatidylcholine (Casal and Mantsch, 1984; Arrondo and Goñi, 1998). Moreover, an intensity decrease of the 1386 cm^{-1} band was also observed, indicating a possible reduction of ergosterol (Levchuk, 1968).

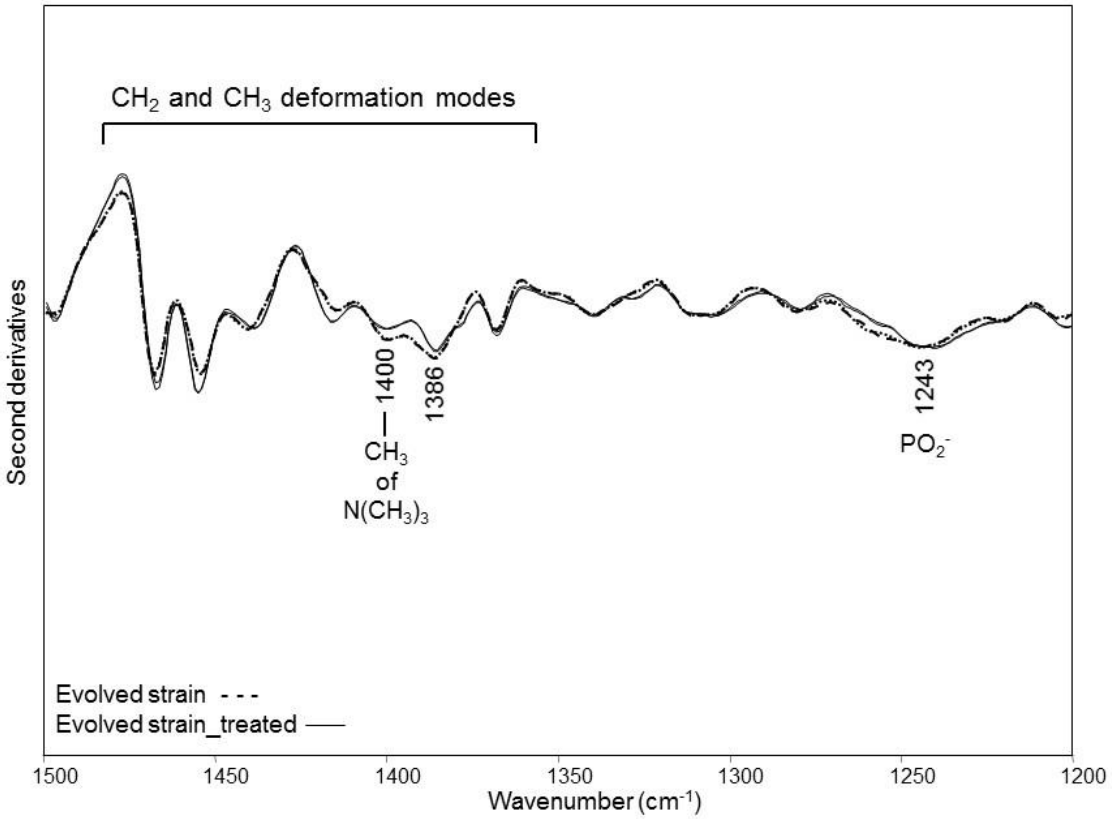

Figure 11. Second derivative analysis between 1500-1200 cm^{-1} of *S. cerevisiae* evolved strain in stationary phase. Second derivative spectra have been reported in the absorption range mainly due to lipid hydrocarbon tails and head groups, after normalization of the absorption spectra at the Amide I band area.

More information on possible lipid variations after acetic acid exposure were given by the analysis of the 3050-2800 cm^{-1} spectral range (Casal and Mantsch, 1984; Arrondo and Goñi, 1998). In particular, as reported in **Figure 12**, in treated cells we found a significant intensity increase of CH_2 absorption mainly at ~ 2851 cm^{-1}, compared to control cells, that indicates a possible rearrangement of the acyl chain length, likely impacting on mebrane fluidity. Furthermore, the shoulder at 2935 cm^{-1} was found to be less intense compared to control cells.

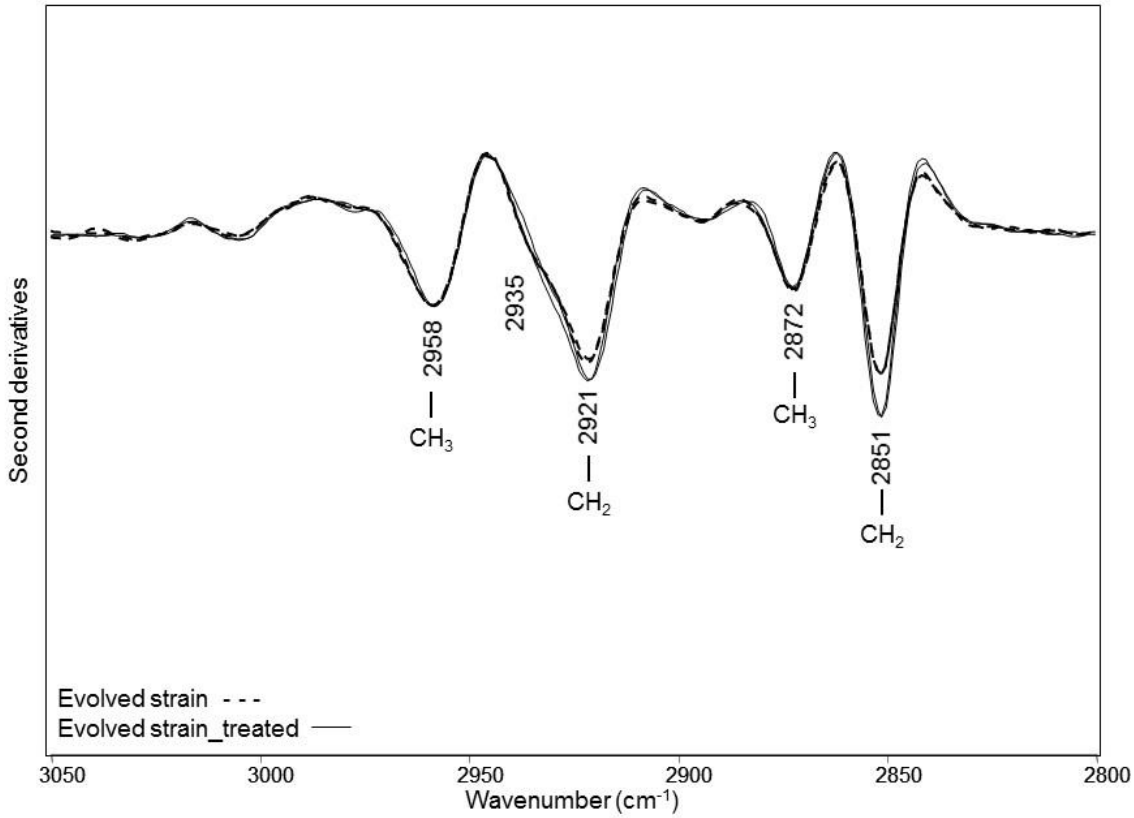

Figure 12. Second derivative analysis of the 3050-2800 cm^{-1} region of *S. cerevisiae* evolved strain in stationary phase. Second derivative spectra have been reported in the absorption range mainly due to CH_3 and CH_2 stretching vibrations of lipid hydrocarbon tails, after normalization of the absorption spectra at the CH_3 band at 2958 cm^{-1}. Two representative spectra for each sample have been reported.

In addition, the infrared response mainly of cell wall carbohydrates is presented in **Figure 13**, between 1200-900 cm^{-1}. As displayed, the complex absorption observed in untreated cells was found to partially change after the treatment with the stressing agent. Specifically, we found an intensity increase of the ~1153 cm^{-1}, ~1080 cm^{-1} and ~1027 cm^{-1} bands that, when simultaneously present, are a marker of glycogen (Naumann, 2000). In addition, the ~1153 cm^{-1} and the ~1080 cm^{-1} are also due to the absorption of β(1-3)glucans, while the ~1027 cm^{-1} band is assigned to β(1-4) glucosidic bonds in chitin or in glucans linked to a N-acetylglucosamine molecule (Galichet *et al.,* 2001; Zimkus *et al.,* 2013). Interestingly, compared to the exponential phase of growth, this complex absorption increased in the treated cells at the stationary phase of growth. Furthermore, the ~ 1043 cm^{-1} absorption detected in control cells and due to mannans was found to upshift to ~ 1047 cm^{-1}, and to increase in intensity. Overall, these spectral features indicate that the exposure to the stressing agent led to

modifications of cell wall components, partially already observed at the exponential phase of growth, like the major intensity of the β (1-6) glucans at 994 cm-^{1} and of the β(1-4) glucosidic bonds at 1027 cm^{-1}.

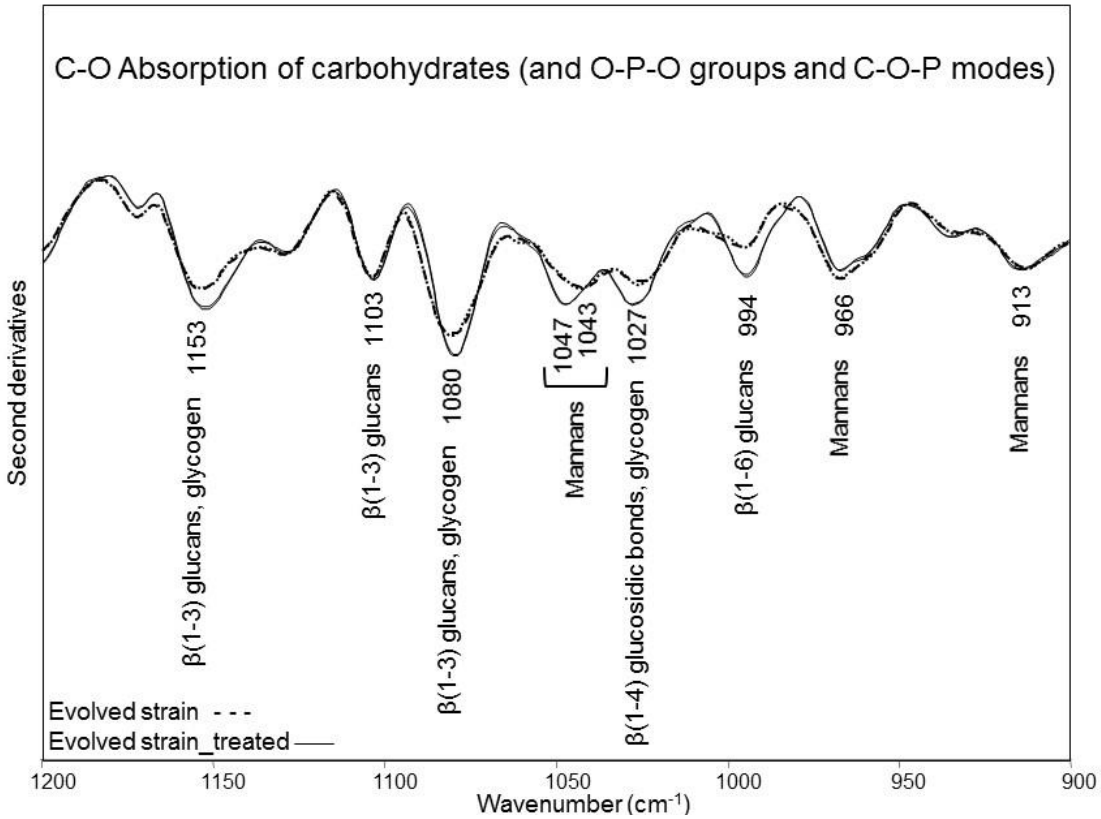

Figure 13. Second derivative analysis of the 1200-900 cm^{-1} region of *S. cerevisiae* evolved strain in stationary phase. Second derivative spectra have been reported in the absorption range mainly due to carbohydrates, after normalization of the absorption spectra at the Amide I band area. Two representative spectra for each sample have been reported.

3.4. SECOND DERIVATIVE ANALYSIS OF THE *S. cerevisiae* MCR1 ENGINEERED EVOLVED STRAIN TREATED WITH ACETIC ACID: STATIONARY PHASE

In **Figure 14**, the infrared absorption of *S. cerevisiae* MCR1 engineered cells treated with acetic acid is compared with untreated cells in the amide I region.

In particular, the second derivative spectrum of the untreated MCR1 cells are characterized by the alpha helix and random coil band at ~ 1656 cm^{-1}, and the intramolecular native beta sheets at ~1637 cm^{-1}. A broad component around 1685 cm^{-}

[1] is also present, likely due to the overlapping absorption of intra/intermolecular beta sheets and beta turns (Tamm and Tatulian, 1997; Barth, 2007).

Specifically, the treatment with acetic acid led to the formation of protein aggregates, as already observed at the exponential phase of growth. Indeed, compared to untreated cells, a new intense band appeared at ~ 1628 cm^{-1}(Seshadri *et al.,* 1999), accompanied by the appearance also of an absorption at ~ 1693 cm^{-1}, both assigned to intermolecular beta sheets. Moreover, a reduction of the intramolecular native beta sheets at ~1637 cm^{-1} has been detected.

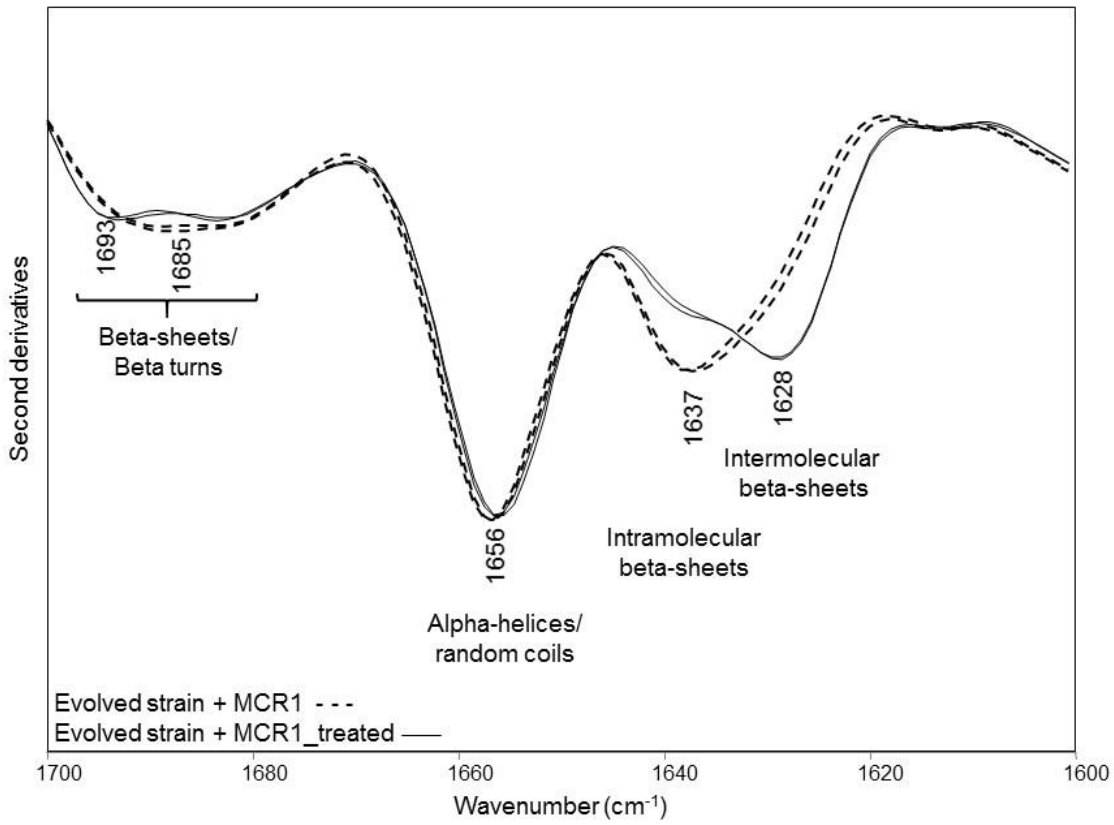

Figure 14. Second derivative spectra of the Amide I region of *S. cerevisiae* MCR1 engineered evolved strain in stationary phase. Second derivative spectra have been obtained after normalization of the absorption spectra at the amide I band area. Two representative spectra for each sample have been reported.

The analysis of the spectral range between 1500- 1200 $cm^{-}1$, reported in **Figure 15**, showed an intensity reduction of the ~1399 cm^{-1} band - due to CH_3 from the $N(CH_3)_3$ - higher compared to the evolved strain – not MCR1 engineered (Casal and Mantsch, 1984; Arrondo and Goñi, 1998). In addition, also a slight but significant reduction of

the ~ 1386 cm^{-1} absorption was observed, that could indicate a decrease of ergosterol (Levchuk, 1968), not detected in the exponential phase of growth.

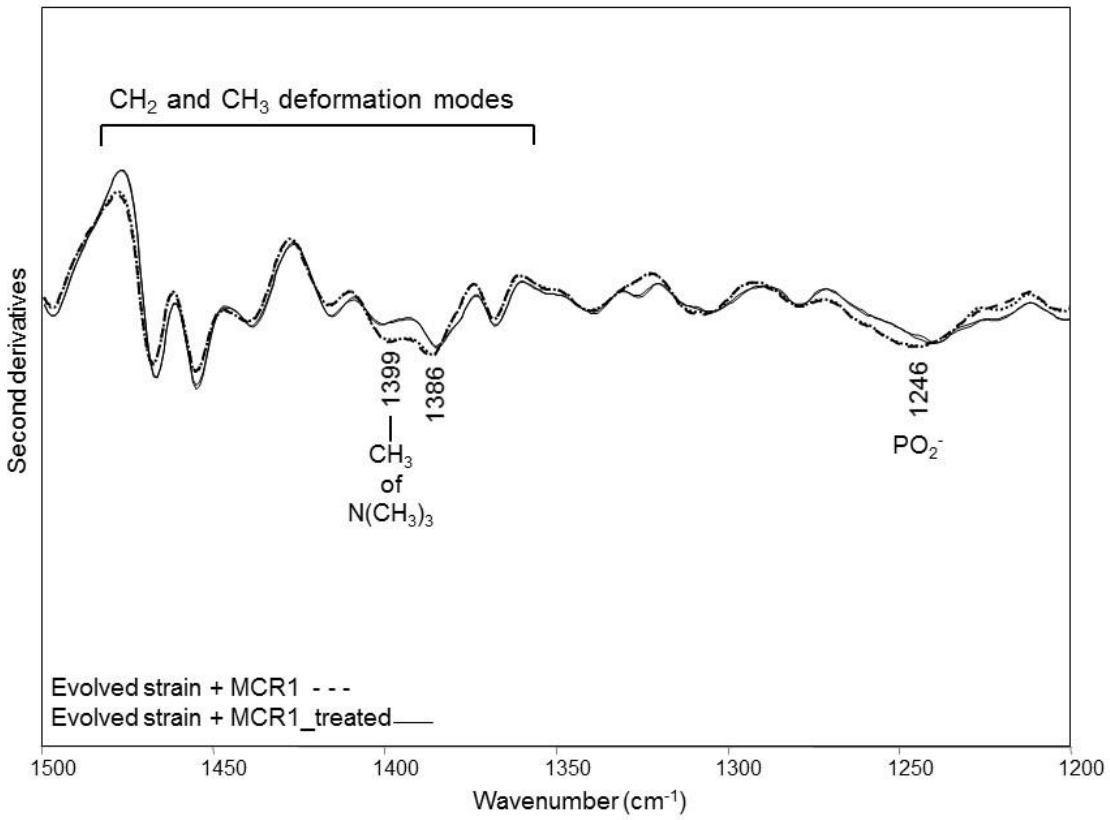

Figure 15. Second derivative analysis between 1500-1200 cm^{-1} of *S. cerevisiae* MCR1 engineered evolved strain in stationary phase. Second derivative spectra have been reported in the absorption range mainly due to lipid hydrocarbon tails and head groups, after normalization of the absorption spectra at the

Moreover, in **Figure 16**, the analysis in the CH_2 and CH_3 stretching region is reported. In particular, compared to the untreated cells, the treatment with acetic acid led to the increase of the intensity of the CH_2 bands, suggesting a possible elongation of the lipid hydrocarbon tails and a possible reduction of the fluidity. Noteworthy, as observed between 1500-1200 cm^{-1}, an important decrease of the ergosterol component around 2935 cm^{-1} was also found.

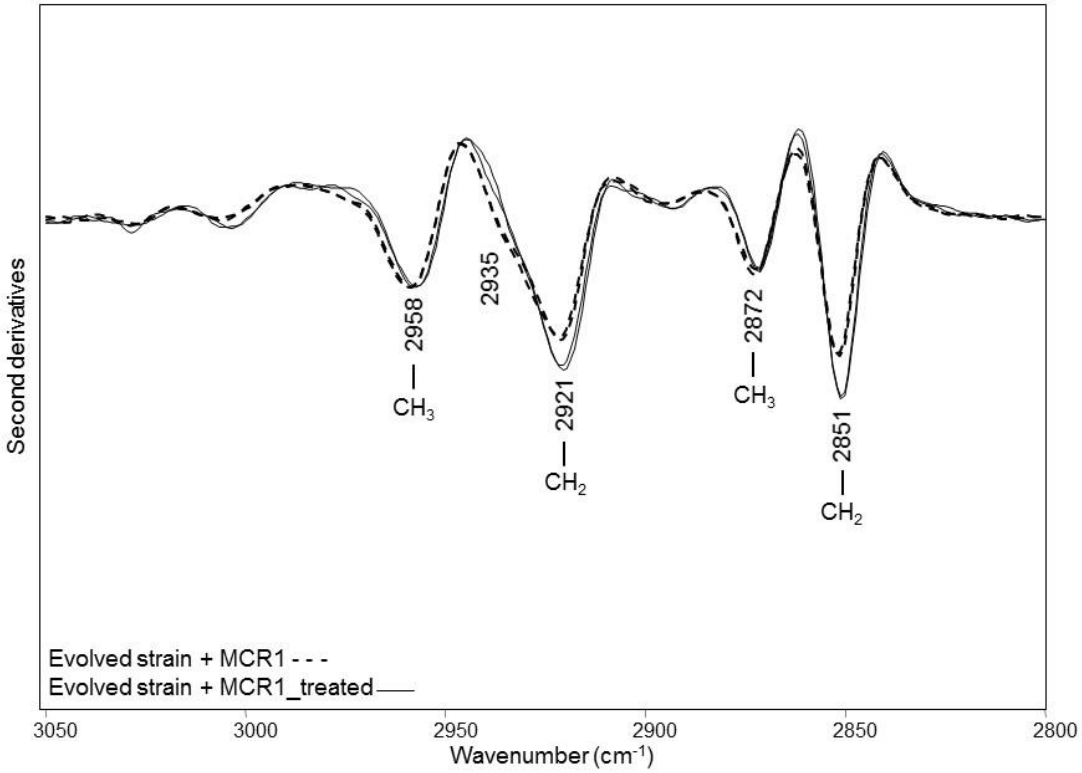

Figure 16. Second derivative analysis of the 3050-2800 cm^{-1} region of *S. cerevisiae* MCR1 engineered evolved strain in stationary phase. Second derivative spectra have been reported in the absorption range mainly due to CH_3 and CH_2 stretching vibrations of lipid hydrocarbon tails, after normalization of the absorption spectra at the CH_3 band at 2958 cm^{-1}. Two representative spectra for each sample have been reported.

Finally, we analyzed the IR response between 1200-900 cm^{-1} in **Figure 17**, and we found, interestingly, very similar results to those obtained for the evolved strain in the stationary phase (see **Figure 13**). In particular, we observed an important intensity increase at ~ 1153 and 1081 cm^{-1} assigned to β(1-3) glucans and at ~ 1027 cm^{-1} due to the absorption of β(1-4) glucosidic bonds (Galichet *et al.*, 2001; Zimkus *et al.*, 2013). In addition, the simultaneous presence of these three bands indicated the presence of glycogen (Naumann, 2000). As detected for the evolved strain in the stationary phase of growth, the β(1-6) glucan band at ~ 994 cm^{-1} was found to increase in intensity, suggesting changes in the complex cell wall network.

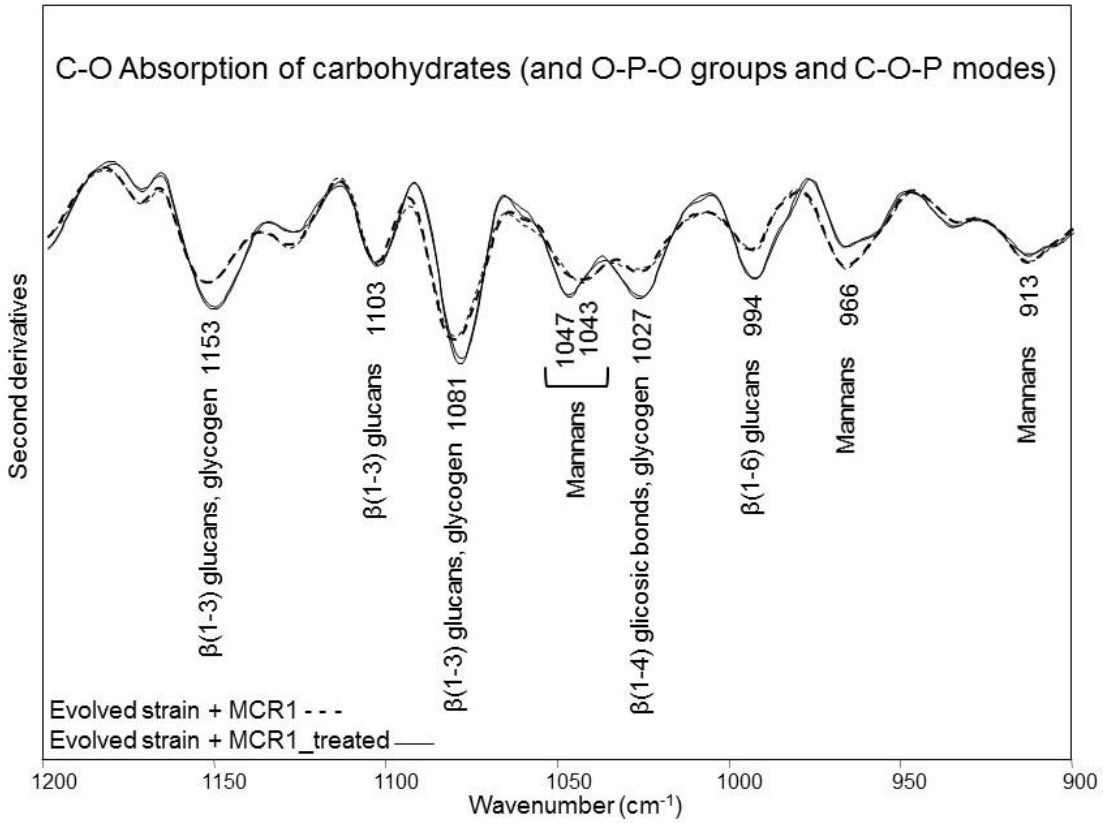

Figure 17. Second derivative analysis between 1200-900 cm^{-1} region of *S. cerevisiae* MCR1 engineered evolved strain in stationary phase. Second derivative spectra have been reported in the absorption range mainly due to carbohydrates, after normalization of the absorption spectra at the Amide I band area. Two representative spectra for each sample have been reported.

4. DISCUSSION AND CONCLUSIONS

When *S. cerevisiae* cells from evolved strain (our control) were challenged with acetic acid, a few changes in the infrared response have been observed compared to untreated cells, starting from the exponential phase of growth. In particular, we detected the appearance of protein aggregation, as expected considering the pH decrease induced by acetic acid. Furthermore, a partial rearrangement mainly of membrane lipids was found, including the decrease of phosphatidylcholine, a slight reduction of ergosterol, as well as an elongation of the lipid acyl chains. Specifically, the modifications of membrane lipid composition, impacting on their physico-chemical properties, could represent a strategy adopted by cells to counteract the acetic acid entrance. Noteworthy, phosphatidylcholine is one of the most important phospholipids that is responsible for membrane fluidity (Fajardo *et al.*, 2011), and it is frequently associated to ergosterol in specific membrane domains (Naumowicz and Figaszewski, 2005). In addition to membrane lipid modifications, also a variation of cell wall carbohydrate components, including in particular glucans, was detected.

Going on to the stationary phase of growth, a further protein aggregation took place in cells treated with acetic acid, accompanied by a higher lipid acyl chain elongation compared to the exponential phase of growth. Surprisingly, we should note that in stationary phase we detected an appreciable amount of protein aggregates also in untreated cells - lower compared to treated cells - that can be a consequence of oxidative stress due to cell aging. Moreover, the cell treatment with acetic acid led to additional changes of the cell wall components, such as an important intensity increase of the beta glucans bands, indicating a thickening of the cell wall that – together with the modifications of the lipid components – could maintain the cells resistant to the stressing agent.

The overexpression of MCR1 gene, that plays a key role in the response to oxidative damage, induces the synthesis of the mitochondrial NADH-cytochrome b5 reductase, and is involved in the synthesis of ergosterol. In particular, its overexpression in *S. cerevisiae* cells makes them more resistant to stressing agents, such as acetic acid. For instance, one important evidence of the stress induced by the presence of acetic acid is represented by the prolonged lag phase which increased from 6 hours in untreated

cultures to 24 hours in cells exposed to the stressing agent (our experiments and Lindberg *et al.*, 2013).

The infrared analysis performed on *S. cerevisiae* cells engineered with MCR1 indicated that in exponential phase of growth the treatment with acetic acid induced the formation of protein aggregates, even if lower compared to the evolved control strain. Moreover, in stationary phase we didn't detect protein aggregates in untreated cells as a consequence of aging, as instead found in the evolved untreated strain. This first result could suggest a role of MCR1 overexpression in counteract the oxidative stress.

The exposure to acetic acid induced also in MCR1 engineered strain a few cell modifications deployed by cells to limit the effects of the stressing agent. Interestingly, these strategies are different to those observed in the evolved strain during exponential phase. In particular, a strong reduction of phosphatidylcholine was detected, more important than in the evolved, not engineered strain. Noteworthy, we didn't observe any reduction of the ergosterol absorption compared to untreated cells, contrarily to what found in the evolved, nor a modification of lipid acyl chain length. Overall these results suggest that MCR1 cells adopt mainly, as a strategy to prevent acetic acid entrance, the increase of ergosterol to decrease membrane fluidity (Endo *et al.*, 2009). In addition, our FTIR results indicated that also the cell wall carbohydrate composition was affected by the stressing agent treatment. In particular, in the exponential phase of growth a reduction of glucans was detected compared to untreated cells, suggesting a reorganization of the complex cell wall network, which will continue in the stationary phase. Indeed, as reported in literature, some genes involved in the tolerance to acetic acid also regulate carbohydrate metabolism, including the synthesis of mannans, β(1-3) and β(1-6) glucans, and chitin (Bulik *et al.*, 2003; Mira *et al.*, 2010).

As anticipated above, cell modifications were still detected in the stationary phase. Noteworthy, however, the strategy adopted by cells appears to be different to that observed in the exponential phase. In particular, to face the effects induced by the exposure to acetic acid, cells were found to modify membrane fluidity by the elongation of acyl chain length rather than by the increase of ergosterol and/or by a strong reduction of phosphatidylcholine. Furthermore, to make the cells more robust also an increase of beta glucan content took place, as found in the evolved strain.

Overall our infrared study firstly suggests that all the modifications adopted by *S. cerevisiae* cells to limit the negative effects induced by acetic acid vary between the phases of growth (Galichet *et al.*, 2001). In particular, in the exponential phase, cells engineered with MCR1 likely counteract the effects of acetic acid by decreasing membrane fluidity, mainly through the dramatic reduction of phosphatidylcholine and the increase of ergosterol, whose synthesis is also regulated by MCR1. Moreover, the engineered cells highlighted a role for the MCR1 gene in counteracting the effects of oxidative stress during aging in the stationary phase of growth. In fact, in MCR1 cells, protein aggregation due to aging didn´t occur, conversely to what observed in the evolved strain.

5. BIBLIOGRAPHY

1. Ami, D., Natalello, A., Doglia, S.M. 2012. Fourier transform infrared microspectroscopy of complex biological systems: from intact cells to whole organisms. Methods. Mol. Biol. 895: 85-100.
2. Arrondo, J.L., Goñi. F.M. 1998. Infrared studies of protein-induced perturbation of lipids in lipoproteins and membranes. Chem. Phys. Lipids. 96: 53-68
3. Banyay, M., Sarkar, M., Gräslund A. 2003. A library of IR bands of nucleic acids in solution. Biophys. Chem. 104(2): 477-488.
4. Barth, A. 2007. Infrared spectroscopy of proteins. Biochim. Biophys. Acta. 1767(9): 1073-1101.
5. Bulik, D.A., Olczak, M., Lucero, H.A., Osmond, B.C., Robbins, P.W., Specht, C.A. 2003. Chitin synthesis in *Saccharomyces cerevisiae* in response to supplementation of growth medium with glucosamine and cell wall stress. Eukaryot. Cell. 2(5): 886-900.
6. Casal, H.L., Mantsch, H.H. 1984. Polymorphic phase behaviour of phospholipid membranes studied by infrared spectroscopy. Biochim. Biophys. Acta. 779(4): 381-401.
7. Chen, Q., Ding, Q., Keller, J.N. 2005. The stationary phase model of aging in yeast for the study of oxidative stress and age-related neurodegeneration. Biogerontology. 6: 1-13.
8. Endo, A., Nakamura, T., Shima, J. 2009. Involvement of ergosterol in tolerance to vanillin, a potential inhibitor of bioethanol fermentation, in *Saccharomyces cerevisiae*. FEMS Microbiol. Lett. 299(1): 95-9.
9. Fajardo, V.A., McMeekin, L., LeBlanc, P.J. 2011. Influence of phospholipid species on membrane fluidity: a meta-analysis for a novel phospholipid fluidity index. J. Membrane Biol. 244: 97-113.
10. Galichet, A., Sockalingum, G.D., Belarbi, A., Manfait, M. 2001. FTIR spectroscopic analysis of *Saccharomyces cerevisiae* cell walls: study of an anomalous strain exhibiting a pink-colored cell phenotype. FEMS Microbiol. Lett. 197: 179-186.

11. Kacuráková, M., Mathlouthi, M. 1996. FTIR and laser-Raman spectra of oligosaccharides in water: characterization of the glycosidic bond. Carbohydr. Res. 284: 145-157.
12. Lee, J.S., Huh, W.K., Lee B.H., Baek, Y.U., Hwang, C.S., Kim, S.T., Kim, Y.R., Kang, S.O. 2001. Mitochondrial NADH-cytochrome b(5) reductase plays a crucial role in the reduction of D-erythroascorbyl free radical in *Saccharomyces cerevisiae*. Biochim. Biophys. Acta. 1527: 31-38.
13. Lesage, G., Bussey, H. 2006. Cell Wall Assembly in *Saccharomyces cerevisiae*. Microbiol. Mol. Biol. Rev. 70(2): 317–343.
14. Levchuk, Y.N. 1968. Infrared Spectra of Steroids. Russ. Chem. Rev. 37(2): 155-171.
15. Lindberg, L., Santos, A.X.S., Riezman, H. Olsson, L., Bettiga, M. 2013. Lipidomic profiling of *Saccharomyces cerevisiae* and *Zygosaccharomyces bailii* reveals critical changes in lipid composition in response to acetic acid stress. PLoS One. 8(9): e73936.
16. Meineke, B., Engl, G., Kemper, C., Vasiljev-Neumeyer, A., Paulitschke, H., Rapaport, D. 2008. The outer membrane form of the mitochondrial protein Mcr1 follows a TOM-independent membrane insertion pathway. FEBS Lett. 582: 855-860.
17. Michell, A.J., Sourfield, G. 1970. An assessment of Infrared spectra as indicators of fungal cell wall composition. Aust. J. biol. Sci. 23: 345-360.
18. Mira, N.P., Palma, M., Guerreiro, J.F., Sá-Correia, I. 2010. Genome-wide identification of *Saccharomyces cerevisiae* genes required for tolerance to acetic acid. Microb. Cell. Fact. 9: 79.
19. Naumann, D. 2000. Infrared Spectroscopy in Microbiology, in: Meyers, R.A., (Ed.). Encyclopedia of Analytical Chemistry, John Wiley & Sons Ltd, Chichester, pp. 102-131.
20. Naumowicz, M., Figaszewski, Z.A. 2005. Impedance analysis of lipid domains in phosphatidylcholine bilayer membranes containing ergosterol. Biophys. J. 89(5): 3174-82.
21. Seshadri, S., Khurana, R., Fink, A.L. 1999. Fourier transform infrared spectroscopy in analysis of protein deposits. Methods Enzymol. 309: 559-576.

22. Squier, T.C. 2001. Oxidative stress and protein aggregation during biological aging. Exp. Gerontol. 36(9):1539-50.
23. Susi, H., Byler, D.M. 1986. Resolution-enhanced Fourier transform infrared spectroscopy of enzymes. Methods. Enzymol. 130: 290–311.
24. Tamm, L.K., Tatulian, S.A. 1997. Infrared spectroscopy of proteins and peptides in lipid bilayers. Q. Rev. Biophys. 30: 365-429.
25. Wallace-Salinas, V., Signori, L., Li, Y.Y., Ask, M., Bettiga, M., Porro, D., Thevelein, J.M., Branduardi, P., Foulquié-Moreno, M.R., Gorwa-Grauslund, M. 2014. Re-assessment of YAP1 and MCR1 contributions to inhibitor tolerance in robust engineered *Saccharomyces cerevisiae* fermenting undetoxified lignocellulosic hydrolysate. AMB Express. 4: 56.
26. Zimkus, A., Misiūnas, A., Chaustova, L. 2013. Li+ effect on the cell wall of the yeast *Saccharomyces cerevisiae* as probed by FT-IR spectroscopy. Cent. Eur. J. Biol. 8(8): 724-728.